

CONSTRAINTS ON THE BINARY COMPANION TO THE SN IC 1994I PROGENITOR

SCHUYLER D. VAN DYK¹, SELMA E. DE MINK², AND EMMANOUIL ZAPARTAS²
Accepted to appear in ApJ.

ABSTRACT

Core-collapse supernovae (SNe), marking the deaths of massive stars, are among the most powerful explosions in the Universe, responsible, e.g., for a predominant synthesis of chemical elements in their host galaxies. The majority of massive stars are thought to be born in close binary systems. To date, putative binary companions to the progenitors of SNe may have been detected in only two cases, SNe 1993J and 2011dh. We report on the search for a companion of the progenitor of the Type Ic SN 1994I, long considered to have been the result of binary interaction. Twenty years after explosion, we used the *Hubble Space Telescope* to observe the SN site in the ultraviolet (F275W and F336W bands), resulting in deep upper limits on the expected companion: F275W > 26.1 mag and F336W > 24.7 mag. These allows us to exclude the presence of a main sequence companion with a mass $\gtrsim 10 M_{\odot}$. Through comparison with theoretical simulations of possible progenitor populations, we show that the upper limits to a companion detection exclude interacting binaries with semi-conservative (late Case A or early Case B) mass transfer. The limits tend to favor systems with non-conservative, late Case B mass transfer with intermediate initial orbital periods and mass ratios. The most likely mass range for a putative main sequence companion would be $\sim 5\text{--}12 M_{\odot}$, the upper end of which corresponds to the inferred upper detection limit.

Subject headings: supernovae: individual (SN 1994I) — galaxies: individual (NGC 5194) — binaries (including multiple): close — stars: massive — stars: evolution

1. INTRODUCTION

Supernovae (SNe) are among the most powerful explosions in the Universe. They are a responsible for the main enrichment of chemical elements and a crucial source of feedback affecting the formation of galaxies. SNe are divided into thermonuclear events (the Type Ia SNe) and those arising from core collapse at the end of a massive star's life (initial mass $M_{\text{ini}} \gtrsim 8 M_{\odot}$). Among the core-collapse SNe are those that are explosions with much or all of the star's hydrogen envelope remaining intact, the Type II SNe, and several types for which the major part of the star's envelope has been stripped away prior to explosion: the Type IIb (showing only traces of H), Type Ib (showing little-to-no traces of H, only of helium) and Type Ic (showing little-to-no traces of H or He). These latter three types are often referred to as "stripped-envelope" SNe.

The H-poor, Type Ib/c SNe comprise $\sim 19\%$ of all SNe (Li et al. 2011) and $\sim 26\%$ of all core-collapse SNe (Smith et al. 2011), implying that they provide an important contribution to galactic chemical evolution. A strong link for these SNe with the evolution of binary systems has been proposed, and their rates currently serve as absolute upper limits for the predicted detection rates of gravitational wave sources (Kim et al. 2010), which may be detected with the new detectors that are now coming online (Aasi et al. 2013). A subclass of these H-poor SNe (the Type Ic-bl) has been connected to long-duration γ -ray bursts (e.g., Woosley & Bloom 2006), which serve as star formation indicators at cosmological distances and probes of the intervening space.

It is therefore fundamental to determine the stellar origins of these SNe.

Unlike for the Type II SNe, despite valiant searches of pre-explosion imaging data (e.g., Barth et al. 1996; Van Dyk et al. 2003; Gal-Yam et al. 2005; Maund et al. 2005; Crockett et al. 2007, 2008; Eldridge et al. 2013; Elias-Rosa et al. 2013), no direct identification has yet been made of the progenitor star, or stellar system, for any SN Ib or Ic, with the possible exception of the SN Ib iPTF13bvn (Cao et al. 2013). The fact that, for SNe Ib and SNe Ic, the H envelope must be highly-to-entirely stripped prior to explosion has led to two main progenitor scenarios. In the first scenario, stellar winds or eruptions, or both, are responsible for the removal of the envelope. This only works for relatively high-mass stars ($M_{\text{ini}} \gtrsim 20\text{--}30 M_{\odot}$ at solar metallicity) that are luminous enough to drive strong winds or have unstable envelopes (e.g., Woosley et al. 1993; Georgy et al. 2009). In this scenario the progenitor is a hot Wolf-Rayet star (e.g., Tramper et al. 2015). In the second scenario, the star loses its envelope through interaction with a binary companion. This scenario applies to a wider range of initial masses. The typical direct progenitor of the SN is a He star of $\approx 2\text{--}4 M_{\odot}$, probably still accompanied by a companion star (e.g., Podsiadlowski et al. 1992; Woosley et al. 1995; Pols & Dewi 2002; Eldridge et al. 2008; Yoon et al. 2010; Claeys et al. 2011; Eldridge et al. 2013). Both scenarios must exist in nature. A larger contribution by the binary scenario is expected, though, because of the high close-binary frequency found for young, massive stars (e.g., Mason et al. 2009; Sana et al. 2012). Secondly, the progenitors include lower-mass stars, which are favored by the initial mass function. We refer to Eldridge et al. (2013) for an overview of arguments in support of both scenarios.

¹ IPAC/Caltech, 100-22, Pasadena, CA 91125 USA

² Anton Pannekoek Astronomical Institute, University of Amsterdam, 1090 GE Amsterdam, The Netherlands

One of the primary impediments to SN Ib/c progenitor detection is reddening. From a systematic examination of SN Ib/c light curves, Drout et al. (2011) found that the mean color excess is $E(B - V) = 0.4 (\pm 0.2)$ mag. Additionally, a number of SNe Ib/c have exceptional amounts of reddening, $E(B - V) \gtrsim 1$ mag, e.g., SNe 2005V and 2005at (Eldridge et al. 2013).

Given how difficult it has been to detect the progenitors of SNe Ib/c, both Eldridge et al. (2013) and Yoon et al. (2012) have suggested returning to the SN site, when the SN has sufficiently faded from view, to search for the companion to the progenitor, if interacting binaries are indeed responsible for these SNe. As Yoon et al. pointed out, the companions should be quite hot, and should therefore best be detectable in the ultraviolet (UV). Such a search, therefore, can only be undertaken with the *Hubble Space Telescope* (*HST*). Binary companions may have been identified in this manner for the Type IIb SNe 1993J (Maund et al. 2004; Fox et al. 2014) and 2011dh (Folatelli et al. 2014; although see Maund et al. 2015). However, detecting a putative companion with *HST* is a non-trivial endeavor, and several factors must be carefully taken into account: The SN must be old enough that it has substantially faded from detectability, especially in the UV; it must have been clearly detected in previous high spatial resolution imaging, ideally also with *HST*; it must have experienced relatively low extinction; it should have occurred in a relatively uncrowded field; and, the SN host galaxy must have a low inclination and also be relatively nearby.

One target that met these various criteria to search for a possible surviving companion is the well-studied SN Ic 1994I. This SN has long been considered as the result of an interacting binary system — see Nomoto et al. (1994) and Iwamoto et al. (1994). The SN occurred $14''.4$ E and $12''.2$ S of the nucleus of NGC 5194 (Messier 51a, also known as the Whirlpool Galaxy). SN 1994I was discovered on 1994 April 2 UT, well before maximum light, with the explosion date likely around 1994 March 27 UT. (UT dates are used hereafter.) The spectral classification was later established by, e.g., Sasaki et al. (1994) and Wheeler et al. (1994). Light curves for the SN were assembled by, e.g., Yokoo et al. (1994), Lee et al. (1995), Richmond et al. (1996), and Clocchiatti et al. (2008). SN 1994I had been held up for years as the “prototypical”, or “standard”, SN Ic (Elmhamdi et al. 2006; Sauer et al. 2006). However, it is evident in hindsight that the SN is atypical in its light curve behavior, relative to other SNe Ic (Richardson et al. 2006; Drout et al. 2011; Bianco et al. 2014), having evolved quite rapidly and been unusually blue in color. Early analyses of the light curves (Iwamoto et al. 1994; Young et al. 1995) pointed toward the explosion of a low-mass ($\sim 2.1 M_{\odot}$) carbon-oxygen core in a star with $M_{\text{ini}} \approx 13\text{--}15 M_{\odot}$. Iwamoto et al. (1994) and Sauer et al. (2006) found that the early blue spectra could be produced by substantial γ -ray heating and mixing of ^{56}Ni ($\sim 0.003\text{--}0.008 M_{\odot}$) in the outer ejecta. Indications from nebular spectra are of a significant low-velocity mass at the progenitor’s dense core, suggestive of a possible aspherical or inhomogeneous explosion (Sauer et al. 2006).

Barth et al. (1996) did not detect a progenitor in *HST* Wide-Field Planetary Camera 1 (WF/PC-1) images from 1992 to an extinction-corrected absolute mag-

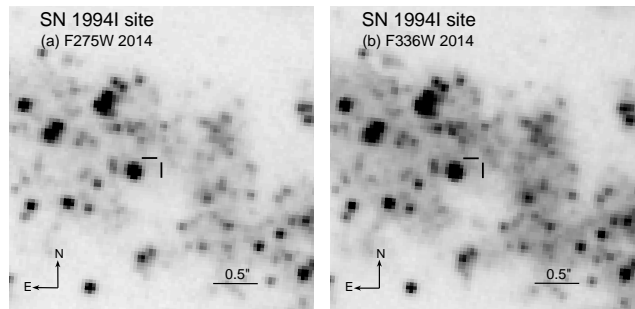


Figure 1. A portion of the WFC3/UVIS images obtained in 2014 September of the SN 1994I site in bands (a) F275W and (b) F336W. The position of the SN in these images is indicated by the tick marks. The rms uncertainty in this position is 0.35 UVIS pixel (13.9 milliarcsec). North is up, and east is to the left.

nitude $M_V^0 \gtrsim -7.3$. A putative binary would most likely have remained undetected, as would an optically less-luminous single WC or WO star.

Here we report on deep observations of the SN site in the ultraviolet obtained more than 20 years after explosion, to search for a hot binary companion, and interpret the results in light of current models for binary star evolution.

2. OBSERVATIONS

The site of SN 1994I was imaged using *HST* with the Wide Field Camera 3 in the UVIS channel on 2014 September 11, under program GO-13340 (PI: S. Van Dyk). These images were obtained in full-array mode in the F275W and F336W bands with total exposure times of 7147 and 4360 sec, respectively. The individual exposures were post-flashed, to a 12-electron level, to mitigate against charge-transfer efficiency (CTE) losses, and also dithered, to mitigate against cosmic-ray hits and bad pixels and to optimize the subpixel sampling of the stellar point-spread function (PSF). The SN site was placed on the more UV-sensitive UVIS chip 2. The images were centered to include as much of the central part of Messier 51a as possible, for lasting archival value, and have been incorporated into the data products offered by the Legacy ExtraGalactic Ultraviolet Survey (LEGUS), an *HST* Treasury program (see Calzetti et al. 2015 for a description of the survey). We display in Figure 1 the portion of the images in each band showing the SN site.

3. DATA ANALYSIS

We first must pinpoint the precise location of SN 1994I in the new *HST* images. Fortunately, *HST* image data exist, obtained in 1994 by GO-5652 (PI: R. Kirshner) of the SN itself using the Wide-Field Planetary Camera 2 (WFPC2) in similar bands, F255W and F336W. The SN was located on the PC chip of WFPC2. We display these images in Figure 2. To establish an astrometric grid, we employed 24 isolated, stellar-like objects in common between the WFPC2 F336W image data from 1994 and the new F336W image. (This band had an overall higher signal-to-noise ratio for both image datasets than did the F255W/F275W ones.) The SN position can be placed in the WFC3 F336W image with an rms uncertainty of 0.35 UVIS pixel (13.9 milliarcsec).

The SN position is indicated in Figure 1. As can be seen from the figure, no source is obviously detected in either WFC3 band.

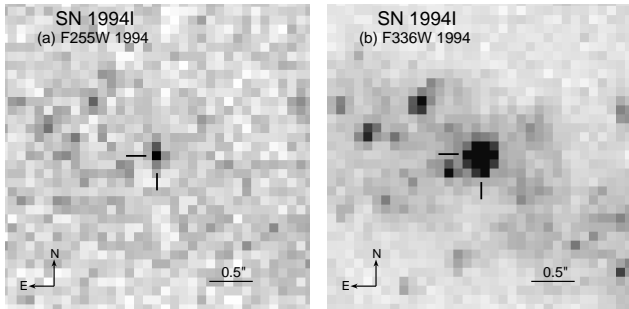


Figure 2. A portion of the WFPC2/PC images of SN 1994I obtained on 1994 May 12 (as part of G0-5652), in (a) F255W and (b) F336W. These images are shown to the same scale and orientation as those in Figure 1. The SN is indicated by the tick marks. North is up, east is to the left.

To establish the detection limit in each of the F275W and F336W bands, we inserted artificial stars at the SN position into the WFC3 images and attempted to detect and measure them above the complex background using Dolphot (Dolphin 2000). However, first, we applied a pixel-based correction to the frames for any CTE losses beforehand, using the routines available for this purpose³. Dolphot was then run on the corrected ‘*flc*’ frames for each band. At F275W we were able to place a detection limit of > 26.1 mag at $\sim 4\sigma$. At F336W the detection limit that we established is > 24.7 mag at $\sim 11\sigma$. As a consequence of the higher detection threshold in this latter band, the F336W data do not provide as stringent of a constraint as do the F275W data. This is likely a result of the overall higher diffuse background around the SN site, as can be seen in Figure 1.

Next we need to make assumptions about the distance and reddening to the SN. Ergon et al. (2014) adopted a distance to M51 of $7.8^{+1.1}_{-0.9}$ Mpc. Vinkó et al. (2012), applying the Expanding Photospheres Method to the two Type II SNe in M51, 2005cs and 2011dh, measured a distance of 8.4 ± 0.5 Mpc (assuming their systematic uncertainty). These two estimates are essentially consistent with each other and with the surface brightness fluctuation (SBF) distance of 7.7 ± 1.0 Mpc (distance modulus 29.42 ± 0.27 mag) measured to M51b by Tonry et al. (2001). We therefore consider here the full range of possible distances to SN 1994I, i.e., 6.7–8.9 Mpc.

The reddening to SN 1994I is likely significant, but relatively uncertain. An estimate of the Galactic foreground extinction contribution can be obtained from Schlafly & Finkbeiner (2011) to be $A_V = 0.096$ mag, i.e., $E(B - V) = 0.031$ mag. From model fits to the early-time light curves, Iwamoto et al. (1994) arrive at $A_V = 1.4 \pm 0.25$ mag ($E[B - V] = 0.45 \pm 0.08$ mag). From model fits to the early spectra, Baron et al. (1996) found $E(B - V) = 0.29$ – 0.45 mag. From further detailed theoretical modeling of early-time spectra, Sauer et al. (2006) concluded that the reddening had to be $E(B - V) = 0.30 \pm 0.05$ mag. Richmond et al. (1996) assumed $E(B - V) = 0.45 \pm 0.16$ mag (or $A_V = 1.4 \pm 0.5$ mag). In an analysis of early-time $V - R$ colors of SNe Ib/c Drout et al. (2011) assumed the Richmond et al. (1996) value for the reddening. Once corrected for this reddening, the color curve for SN 1994I becomes among

Table 1
Brightness Ranges for Hot Dwarf Stars^a

Spectral Type	T_{eff} (K)	M_V^0 (mag)	F275W Range (mag)	F336W Range (mag)
O5V	41000	−5.7	22.34–24.24	22.69–24.33
O8V	35000	−4.9	23.22–25.12	23.54–25.19
B0V	30000	−4.0	24.23–26.13	24.54–26.19
B1V	25400	−3.6	24.86–26.76	25.11–26.75
B3V	18700	−1.6	27.29–29.18	27.42–29.06

^a Based on Castelli & Kurucz (2003) model stellar atmospheres. Assumes that the distance to the stars is in the range of 6.7–8.9 Mpc and that the reddening $E(B - V)$ is in the range of 0.25–0.45 mag. Also assumes a Cardelli et al. (1989) reddening law.

the bluest in their sample. Finally, we mention that, from a high-resolution SN spectrum, Ho & Filippenko (1995) concluded that $A_V = 3.1^{+3.1}_{-1.5}$ mag. Such a high reddening implies both an observed SN and the conditions leading up to the explosion that are astrophysically unrealistic. Ho & Filippenko (1995) noted that their estimate seemed excessively large, relative to the other reddening indicators, which pointed to $A_V \lesssim 1.4$ mag. Here we adopt a range in reddening of $E(B - V) = 0.25$ – 0.45 mag (from the low end of the Sauer et al. 2006 estimate to the value assumed by Drout et al. 2011, since dereddening the color curve by more than this leads to colors that are excessively and possibly unphysically blue). We are, of course, assuming that the reddening to the SN site is equal to the reddening to the SN itself.

With these assumed ranges in distance and reddening to SN 1994I, we can compute what would be the observed brightnesses of hot stars with various effective temperatures and luminosities (and, therefore, masses) and compare these to the WFC3 detection limits. We have assumed that the stars would effectively be dwarfs (equivalent to main sequence stars; see discussion below). We accomplish this using STSDAS/SYNPHOT within PyRAF⁴ and the Castelli & Kurucz (2003) model stellar atmospheres. We also assumed the Cardelli et al. (1989) reddening law. The resulting stellar brightness ranges for stars with various effective temperatures T_{eff} and absolute magnitudes M_V^0 are listed in Table 1.

We show these allowed ranges in brightness, together with the magnitude limits on the WFC3 images at the SN site, in Figure 3. Interpolating from this figure and Table 1, a star hotter than about B2, i.e., $T_{\text{eff}} \gtrsim 23000$ K, and more luminous than $L_{\text{bol}} \approx 10^{3.6} L_{\odot}$ would have been detected. A by-eye comparison of such a star’s temperature and luminosity to the theoretical massive-star evolutionary tracks with rotation from Ekström et al. (2012) implies that a detected star would have $M \gtrsim 10 M_{\odot}$. Therefore, any putative companion to the SN 1994I progenitor would have had $M \lesssim 10 M_{\odot}$.

We note that the late-time luminosity of the SN could be complicated by interaction of the SN shock with its circumstellar medium. Such interaction can lead to emission at radio, X-ray, UV, and optical wavelengths (e.g., Chevalier 1984; Chevalier & Fransson 1994). In fact, Weiler et al. (2011) and Alexander et al. (2015) de-

³ Anderson, J., 2013, http://www.stsci.edu/hst/wfc3/tools/cte_tools.

⁴ STSDAS and PyRAF are products of the Space Telescope Science Institute, which is operated by AURA for NASA.

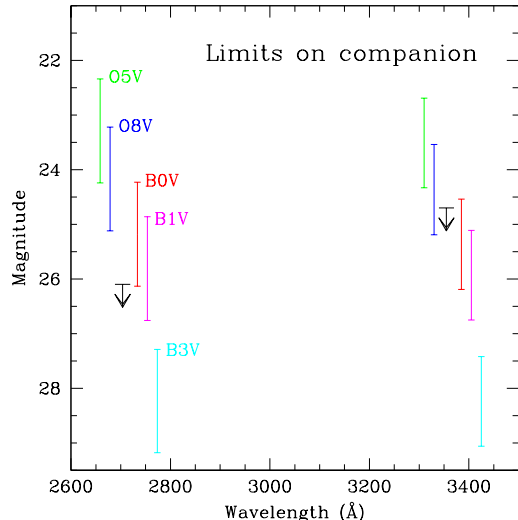


Figure 3. The limits on the detection of a putative companion to the progenitor of the SN 1994I, estimated from the *HST* WFC3/UVIS data at F275W and F336W. Also shown are the ranges in possible observed brightness for main sequence dwarfs of types O5V–B3V, given in Table 1, assuming that the distance to the stars is in the range of 6.7–8.9 Mpc and that the reddening $E(B - V)$ is in the range of 0.25–0.45 mag, and a Cardelli et al. (1989) reddening law. The representations of the various stellar types are shifted somewhat in wavelength in the figure for the sake of clarity.

tected and analyzed the radio synchrotron emission from SN 1994I. X-ray emission was also detected from SN 1994I up to 7 years after explosion (Immler et al. 1998, 2002). Rampadarath et al. (2015) analyzed *Chandra* X-ray Observatory ACIS-S 667-ks observations of the host galaxy from 2012 September (PI: K. Kuntz) and concluded that SN 1994I was still emitting at X-rays, although these authors did not detect it in sensitive radio VLBI imaging from 2011. This is odd, if for SNe Ic we expect the X-ray emission to be the high-energy tail of the synchrotron emission generated by the interaction (Chevalier & Fransson 2006). We have also analyzed the deep *Chandra* data from 2012 and suspect that the X-ray source, detected in a complex region of X-ray emission from the host galaxy, is not actually associated with the SN (the absolute radio position of the SN is not exactly coincident with the radio source), although obviously no pre-SN *Chandra* observations are available to confirm this. Nonetheless, we consider the presence of late-time circumstellar interaction to be unlikely.

Additionally, the amount of reddening to the SN could be further complicated by the formation of dust in the ejecta at late times. Although images of the SN site obtained with the *Spitzer Space Telescope* are spatially too confused to ascertain whether the SN has ever been a source of infrared emission, the host galaxy was observed by *HST* with WFC3/IR in the F110W ($\sim J$) band in 2013 September (PI: J. Koda). We accurately registered these images to the WFPC2 images of the SN in F814W (also by Kirshner), to a 1σ uncertainty of 0.2 WFC3/IR pixels. Nothing is detected in the infrared at this position. We measured photometry from these data, also using Dolphot, and estimate a very low upper limit to detection of 23.8 mag (at $\sim 6\sigma$), or $\approx 0.5 \mu\text{Jy}$. We therefore consider the likelihood of excess dust extinction to

be low. If the SN were somehow additionally reddened at, say, the $\sim 10\%$ level, this would not affect our conclusions here. We would still place a mass limit on a companion at $10 M_{\odot}$. However, if additional reddening were $\sim 20\%$, the star would then have to be hotter than B1V and the inferred mass limit would be at $\gtrsim 17 M_{\odot}$.

4. INTERPRETATION

4.1. Comparison with the original predictions by Nomoto et al. (1994)

Not long after the discovery of SN 1994I, Nomoto et al. (1994) argued that a single star scenario, where the envelope is removed by stellar winds, is inconsistent with the rapid decline of the light curve. The single-star scenario predicts massive C- and O-rich stars as progenitors. A high-mass progenitor would imply considerably longer light curve decline times than observed.

Instead, Nomoto et al. (1994) proposed three possible binary scenarios to explain the observed properties of SN 1994I. Those authors did not present simulations for these scenarios, but they did provide quantitative arguments to estimate the relative contribution of the scenarios. They concluded that the three scenarios are roughly equally as likely. (We draw a different conclusion based on our new simulations, as discussed below in Section 4.2.)

In all three scenarios the SN progenitor is stripped by a companion in two subsequent stages. The first stage removes the H envelope and leaves behind a naked He star with $M \lesssim 4 M_{\odot}$. Such low-mass He stars expand substantially during the He shell burning phase and can reach sizes of tens of solar radii. The expansion can cause them to fill their Roche lobe a second time, now removing a large fraction of the He layers.

The three scenarios differ with respect to the type of the companion. In Path A the SN results from the primary, i.e., the initially more massive star. The companion is a low-mass main sequence star ($1\text{--}4 M_{\odot}$). The high mass ratio at the onset of the first Roche lobe overflow ensures highly non-conservative mass transfer. In Paths B and C the SN Ic results from the secondary, i.e., the initially less massive star. For both of these latter two paths the primary evolves first and leaves behind a compact remnant: either a neutron star for Path B or a white dwarf for Path C. In both cases the compact remnant of the primary strips the original secondary star of most of its He.

Our upper limits on the presence of a companion are consistent with all three binary evolutionary paths from Nomoto et al. (1994). A low-mass ($1\text{--}4 M_{\odot}$) main sequence companion (Path A) is well within the observed upper limits. Also a neutron star or white dwarf companion (Path B and C) would not be detectable, based on our *HST* data.

4.2. Comparison with new population synthesis predictions

To reassess the original predictions by Nomoto et al. (1994) and to provide a theoretical framework to put our new upper limits in perspective, we performed new population synthesis simulations. We aim to investigate the possible progenitor systems that produce “1994I-like” events, as we will define below.

4.2.1. Method and assumptions

We employ the `binary_c` synthetic binary evolutionary code developed by Izzard et al. (2004, 2006, 2009), with updated treatments for the massive binaries as described in de Mink et al. (2013). This code relies on the approximate evolutionary algorithms by Tout et al. (1997) and Hurley et al. (2000, 2002). These algorithms are so fast and robust that they allow predictions to be made for entire populations of massive binaries. At present such simulations are too demanding for detailed binary evolutionary codes, such as MESA (e.g., Paxton et al. 2015); see, however, Eldridge et al. (2008). Future investigation with detailed codes would be desirable, but our method is suitable for the scope of the present study. In a forthcoming paper (Zapartas et al., in preparation) we will present an extended discussion based on these simulations of the impact of binarity on the statistical properties of core-collapse SNe in general. A complete description of the assumptions is provided in de Mink et al. (2013, and references therein). Below, we provide a brief summary of the assumptions for the most relevant physical processes.

We simulate a population of binary stars assuming continuous star formation, choosing initial primary masses, M_1 , from a Kroupa (2001) initial mass function. The companion masses, M_2 , are chosen such that the mass ratio, $q \equiv M_2/M_1$, is distributed uniformly between 0.1 and 1 (e.g., Duchêne & Kraus 2013; Sana et al. 2012). For the initial orbital periods, we assume a uniform distribution in log space (“Öpik’s law;” Öpik 1924). For systems with initial masses above $15 M_\odot$ we adopt the steeper distribution by Sana et al. (2012). We consider initial orbital periods, p , in the range $0.15 \leq \log_{10} p(\text{days}) \leq 3.5$, consistent with Sana et al. (2012). We simulate a grid of $200 \times 200 \times 200$ binary systems, varying the initial masses of both stars and the initial orbital period.

The evolution of the stellar structure follows the detailed evolutionary models by Pols et al. (1998). We account for wind mass loss as described in de Mink et al. (2013), following Vink et al. (2000) and Nieuwenhuijzen & de Jager (1990). For stars that are stripped from their H envelopes, we adopt the Wolf-Rayet mass-loss prescription by Hamann et al. (1995), reduced by a factor of 10 to account for the effect of wind clumping.

The low-mass He stars produced in binaries undergo a very rapid increase in the surface luminosity during their final evolutionary stages (e.g., Yoon et al. 2010, 2012), which is accounted for in our simulations. The mass-loss rate may increase dramatically during this stage to reach $10^{-5} M_\odot \text{yr}^{-1}$, similar to that found for Galactic Wolf-Rayet stars (e.g. Kim et al. 2015), and as implied for many SN Ib/c observations (e.g., Wellons et al. 2012), including SN 1994I, in particular (Alexander et al. 2015). However, the duration of the final phase is very short ($\lesssim 10^4$ years). Therefore, this phase does not have a significant impact on the final masses of the system or on other evolutionary properties that we predict here.

We model the effects of tides on the stellar spins and orbit, following Zahn (1977) and Hurley et al. (2002). We allow for conservative and non-conservative mass transfer and angular momentum, following Hurley et al. (2002). We limit the accretion rate to ten times the thermal mass-transfer rate of the accreting star. Material lost

from the system is assumed to have the specific angular momentum of the orbit of the accreting star. Formation of contact systems and the onset of common-envelope evolution are modeled using critical mass ratios, as detailed in de Mink et al. (2013) and Hurley et al. (2002). Common-envelope evolution is treated by adopting the Webbink (1984) energy balance prescription, using an efficiency parameter, α_{CE} , which is chosen to be unity in our standard simulations. The binding energy of the envelope is taken from Dewi & Tauris (2000). We account for neutron star birth kicks by randomly drawing a scalar velocity from a 1D Maxwellian distribution characterized by width $\sigma = 265 \text{ km s}^{-1}$ (Hobbs et al. 2005).

The observational uncertainties and code limitations do not allow us to distinguish between a SN Ib and SN Ic in our models. We therefore adopt the following approximate criteria. We select explosions in which the progenitor star has lost its entire H-rich envelope. We ensure that the progenitor has also lost a substantial fraction of the He envelope by only selecting systems that experience an additional late phase of Roche-lobe stripping during the He-core or He-shell burning phase. We further explicitly require that the progenitor star is a low-mass He star by selecting final masses for the progenitor in the range $2.2\text{--}4 M_\odot$, to satisfy the constraints originally placed by Iwamoto et al. (1994) and Young et al. (1995).

4.2.2. Relative rates for the different types of companions

We find that 1994I-like SN progenitors, as defined above, are overwhelmingly dominated by systems where the companion star is a main-sequence star at the moment of explosion, at 99% of the events in our standard simulation. We find that cases where the companion is a neutron star or white dwarf are strongly suppressed by our standard assumptions.

This is remarkably different from the estimates made by Nomoto et al. (1994), who expected the three scenarios, A, B and C (in which the companion is a main sequence star, neutron star or white dwarf, respectively) to have a roughly equal likelihood. We identify two reasons for this difference. The first reason is that many systems that could have become 1994I-like progenitors through these paths have extreme mass ratios at the onset of reverse mass transfer. They therefore enter a common envelope phase. With the assumptions used in our simulations, these systems fail to eject the envelope and result in a premature merger. This can be illustrated by the results we obtain when we repeat our simulations using artificially-increased values of the common-envelope efficiency parameter, $\alpha_{\text{CE}} = \{1, 2, 5, 10\}$. This prevents premature mergers and indeed leads to an increase of the relative contribution to 1994I-like events with white dwarf companions, $f_{\text{Path C}} = \{\ll 1\%, 3\%, 31\%, 41\%\}$, respectively, for the assumed values of α_{CE} .

The second reason that we identify as an explanation for the difference is that we account for realistic birth kicks of neutron stars (e.g., Hobbs et al. 2005). Kicks were not considered by Nomoto et al. (1994). The majority of binary systems that could have become 1994I-like progenitors in our simulations dissociate when the first star explodes and leaves behind a neutron star. This, in combination with the premature mergers discussed above, strongly suppresses Path B.

We can reconcile the estimates by Nomoto et al.

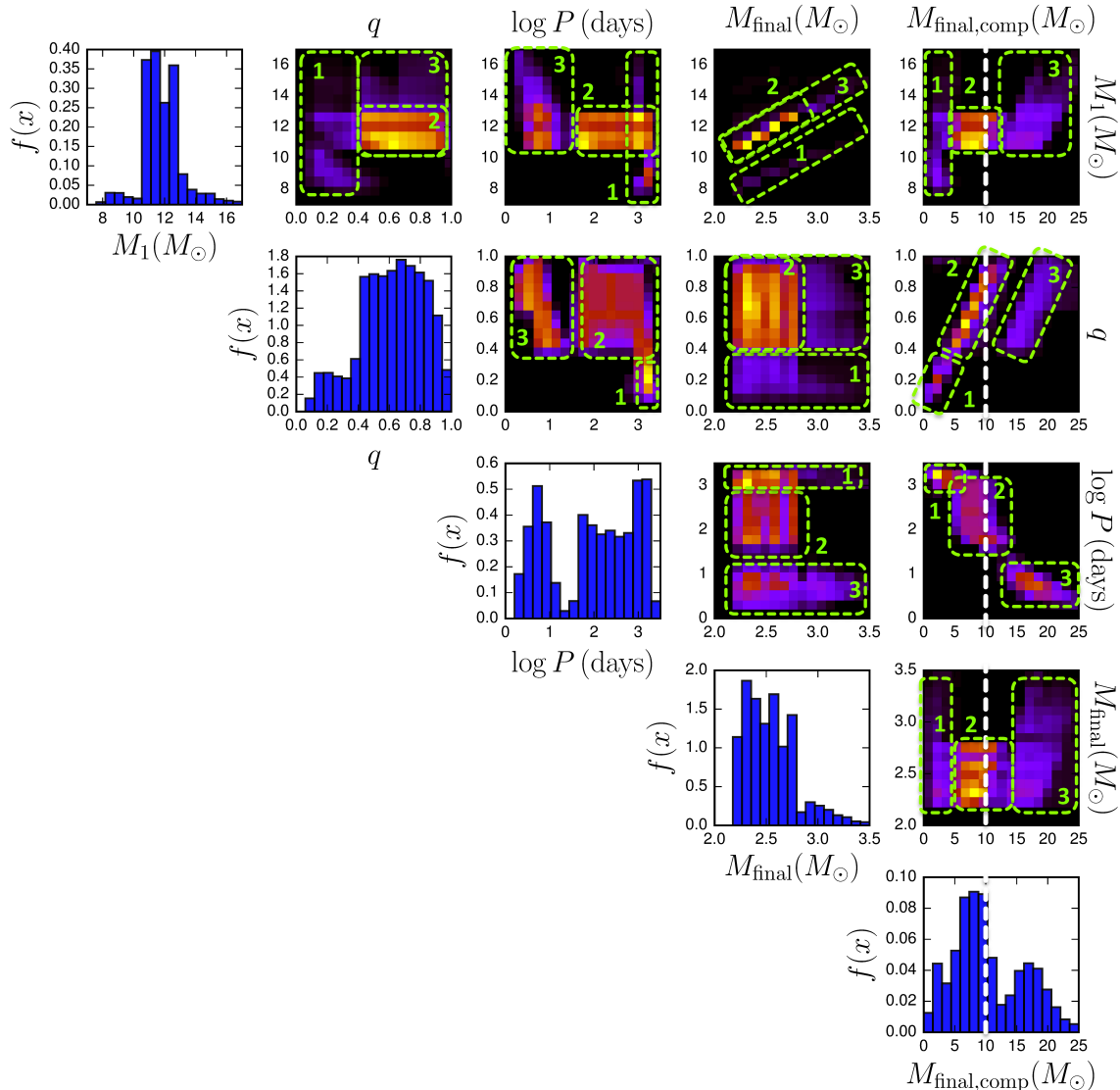


Figure 4. Population synthesis predictions for stripped-envelope SNe with properties similar to SN 1994I (see text for details). Diagrams show the normalized 1D and 2D distributions of the initial primary mass, M_1 , in solar masses; the initial mass ratio, $q = M_2/M_1$; the initial orbital period, p , in days; the final mass of the progenitor before explosion, M_{final} , in solar masses; and, the mass of the companion star at the moment of the SN, $M_{\text{final,comp}}$, in solar masses. For the 2D distributions, the lighter the color shown, the higher the probability density per bin. Approximate regions corresponding to the three scenarios, A-1, A-2, and A-3 (see text), are indicated with green dashed boxes. The inferred upper limit provided by the *HST* observational data presented here, indicated as a vertical, white dashed line in the rightmost panels, excludes all progenitors with $M_{\text{final,comp}} > 10 M_{\odot}$.

(1994), but only by adopting extreme assumptions, which we consider unrealistic. If we fully suppress the birth kicks, i.e., set $\sigma = 0 \text{ km s}^{-1}$, to prevent the break-up of systems, and simultaneously increase the α_{CE} to 10, to prevent premature mergers, we recover relative ratios of $f_{\text{PathA}} = 24\%$, $f_{\text{PathB}} = 24\%$ and $f_{\text{PathC}} = 33\%$, similar to Nomoto et al. (1994), with the remainder coming from a variety of exotic channels. In the discussion below we continue to describe the results for our standard assumptions, where Path A dominates.

4.2.3. Properties of 1994I-like progenitors and expected companions

The most likely companion for 1994I-like events is a main sequence star in our standard simulations. We find that the surviving main-sequence companion does not

need to be as low as $\lesssim 4 M_{\odot}$, as stated by Nomoto et al. (1994). We find many progenitor systems in which the companion is significantly more massive.

In Figure 4 we show the distributions of properties of our simulated progenitor systems. We provide the 1D distributions of the initial parameters describing the binary system, i.e., M_1 , q , and p , together with the final masses of the progenitor, M_{final} , and the companion, $M_{\text{final,comp}}$. In addition, we provide 2D distributions of the correlations between the parameters.

We can distinguish different subgroups of progenitor systems, A-1, A-2 and A-3, in which the companion is increasingly more massive. The green markings in Figure 4 outline the approximate locations of these groups. There are no hard boundaries between these groups, but they are most clearly separated in the panel showing p versus

q (Figure 4, second row and third column). Subgroup A-1 is equivalent to Path A described by Nomoto et al. (1994), and A-2 and A-3 are new. We describe them below. The percentages in parentheses indicate the relative contribution of these channels.

A-1 Long-Period Systems (11%): This subgroup of 1994I-like progenitors originates from binary systems with $p \gtrsim 1000$ days and extreme $q \lesssim 0.4$. These systems are so wide that the primary is an evolved red supergiant when it fills its Roche lobe, initiating highly non-conservative Case C mass transfer. This leads to a common envelope phase. The secondary spirals in, but leads to the ejection of the primary’s H envelope, exposing its naked He core. A second mass-transfer phase occurs when the He star expands during He-shell burning. The secondary does not significantly accrete during the mass-transfer phases. It is still a very low-mass star at the moment of explosion, typically $\lesssim 4 M_{\odot}$ (see Figure 4, rightmost column).

A-2 Intermediate-Period Systems (54%): For intermediate periods, $p \sim 30\text{--}1000$ days, and less extreme mass ratios, $q \gtrsim 0.4$, we find 1994I-like SN progenitors that experience non-conservative, late Case B mass transfer. They result from systems with typical primary masses of $11\text{--}14 M_{\odot}$. Masses for the companion star at the moment of explosion through this channel are typically $\sim 5\text{--}12 M_{\odot}$.

A-3 Short-Period Systems (31%): We also find 1994I-like SNe arising from systems that experience semi-conservative mass transfer, through late Case A or early Case B Roche-lobe overflow, with $p \lesssim 20$ days and $q \gtrsim 0.4$. In this group the companion accretes and retains a large fraction of the H envelope of the primary star. At the moment of explosion of the primary, the companion typically has a mass ranging from $\sim 12\text{--}25 M_{\odot}$.

Our simulations show a fourth subgroup, of extremely close Case A mass-transfer systems which leave behind companions with $\gtrsim 25 M_{\odot}$, accounting for 3% of the total possibilities. However, our population synthesis code cannot adequately follow the core evolution of such close systems that interact very early on the main sequence, and we therefore disregard this minor channel.

4.2.4. Implications of the upper limit on M_{comp} in the framework of the new simulations

The upper limit on the mass of a possible main sequence progenitor, $M_{\text{comp}} < 10 M_{\odot}$, provided by the new data presented in this study, is deep enough to put stringent constraints on our simulations. This can be seen in Figure 4, in which the upper mass limit is marked as a vertical dashed line in the rightmost panels. In total, the upper limit rules out $\sim 44\%$ of the possible evolutionary paths for the progenitor of SN 1994I. It completely excludes the semi-conservative channel (subgroup A-3), which involves a relatively high-mass companion. It also excludes some of the highest-mass companions possible in subgroup A-2. The most likely channel leading to SN

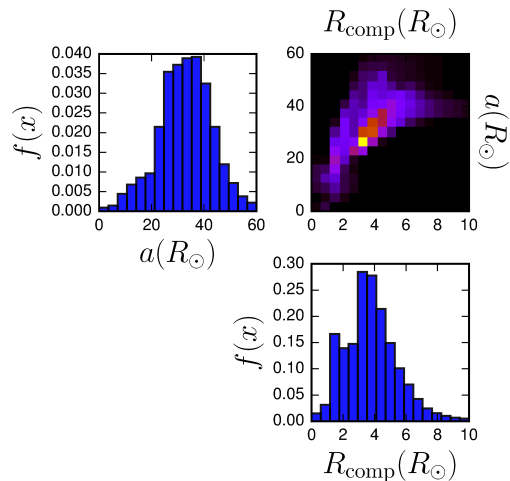


Figure 5. Normalized distributions of final orbital separations, a , and the radii of the companion, R_{comp} , both in solar radii, at the time of explosion. We only show binary progenitor systems that produce SN 1994I-like events. We also applied our observational upper limit on the companion mass, i.e., we only include systems where $M_{\text{final,comp}} < 10 M_{\odot}$. See Figure 4 and the text.

1994I that remains, after applying the upper limit, is A-2, with a most probable companion mass of $\sim 8 M_{\odot}$ at the time of explosion.

We expect the progenitors of 1994I-like SNe Ic to reside in close binary systems when the SN occurs. Our simulations indeed demonstrate this. In Figure 5 we show the distribution of the separation, a , between the progenitor and its companion, and the distribution of the final radii for the companion, R_{comp} , both expressed in R_{\odot} . We also apply the upper limit on the companion mass, requiring that $M_{\text{comp}} < 10 M_{\odot}$. We therefore find that the typical separation is $\sim 30 R_{\odot}$, and the typical radius of the companion at the moment of explosion, R_{comp} , peaks around $\sim 4 R_{\odot}$.

5. DISCUSSION AND CONCLUSIONS

We have conducted deep *HST* UV imaging of the site of the SN Ic 1994I, in order provide constraints on a putative binary companion of the SN progenitor. No companion was detected at the SN site. Our limits appear to exclude any star hotter than about spectral type B2 and, therefore, an inferred mass $\gtrsim 10 M_{\odot}$, assuming the companion would be on the main sequence. These results are consistent with the original predictions for a companion made by Nomoto et al. (1994).

To further investigate the constraining value of these upper limits, we used binary populations synthesis simulations of core-collapse SNe. We analyzed the properties of the systems that will likely result in events similar to SN 1994I, i.e., SNe Ib/c with low-mass progenitors, which have been, at least partially, stripped of their He layers by their companion star.

We recover the three progenitor channels suggested by Nomoto et al. (1994), which predict a main sequence, white dwarf, or neutron star companion at the moment of explosion. In contrast to Nomoto et al. (1994), however, we find that white dwarf and neutron star companion channels are heavily suppressed. In our simulations, many such systems merge prematurely. They fail to eject the common envelope, unless we adopt extreme values for the common envelope efficiency. Secondly, the

inclusion of realistic birth kicks for neutron stars (which were not accounted for by Nomoto et al. 1994) disrupts a large fraction of the potential neutron star companion systems.

For the channels in which the companion is a main sequence star, we identify three subgroups. In addition to the low-mass companions, $\lesssim 5 M_{\odot}$, resulting from highly non-conservative systems as predicted by Nomoto et al. (1994), we find a group of progenitor systems resulting from semi-conservative mass transfer, that leave behind companion stars ranging from 12–25 M_{\odot} , which can be eliminated, based on the observed upper detection limits. A third group is also found, which leave behind companion stars with intermediate masses, ~ 5 –12 M_{\odot} . We consider this latter group to be the most likely.

An aspect to consider for this progenitor system, for which the companion radii are typically $\sim 4 R_{\odot}$ and the close final orbital separations are typically only $\sim 30 R_{\odot}$, is, could the properties of the probable companion be affected by the SN explosion (e.g., Kasen 2010; Moriya et al. 2015; Liu et al. 2015)? We expect that the SN ejecta would reach the companion star within the first hour or so after explosion. From their hydrodynamical simulations, Liu et al. (2015) found that, with typical separations $a \gtrsim 5 R_{\text{comp}}$ (which is likely true in this case), less than 5% of the companion mass is removed by a SN Ib/c impact (relatively high-mass companions have higher surface escape velocities and, so, less mass would be removed), the companion experiences an impact velocity of only a few tens of km s^{-1} , accumulates on its surface only a few $\times 10^{-3} M_{\odot}$ of heavy element-rich ejecta after impact, and, more importantly, and receives heating by the SN which is too inefficient to cause the surviving star to inflate by much (plus, the fractional change in the internal stellar energy produced by the SN shock is smaller, due to the higher internal energy in high-mass stars). So, the properties of the survivor probably did not vary significantly after the explosion, although the binary itself could have been disrupted. Thus, our assumption that the survivor could be approximated 20 years after explosion by a normal main sequence star is probably valid. Furthermore, could SN 1994I have been brightened by the impact on the companion? Moriya et al. (2015) have estimated, using similar population synthesis models, that only about 5 out of 1000 SNe Ib/c should show evidence for brightening at early times. As it is, the earliest detection of SN 1994I was likely already a few days past explosion (Richmond et al. 1996), so any brightening was probably missed.

It is a curious concurrence that the more likely mass range for a companion to the SN 1994I progenitor from our population simulations is ~ 5 –12 M_{\odot} , the upper end of which also happens to correspond to the inferred upper mass limit allowed by our observations. Had we gone even deeper with *HST*, could we have plumbed this mass range further and potentially made a detection of the star? Would such observations had been feasible or realistic? Using the WFC3/UVIS Exposure Time Calculator⁵, and given even the smallest distance and least reddening that we have assumed here, we compute that, to detect a $\sim 5 M_{\odot}$ main sequence star at signal-to-noise

ratio of ~ 5 would require ridiculous exposure times of $\sim 181,000$ sec at F275W and $\sim 60,000$ sec at F336W. Even to go down midway in this mass range, to detect a $\sim 8 M_{\odot}$ star, would require ~ 22000 sec and ~ 10890 sec, respectively. These are ~ 3 and ~ 2.5 times deeper than we had already observed, requiring about 12 orbits of spacecraft time, though, this would not be a completely unreasonable observing request. However, the situation would only get worse if SN 1994I is farther away and more reddened (as we discussed above). So, we may have probably done just about as well as we could have, observationally, to search for a SN 1994I progenitor companion. Additionally, the list of other possible targets that meet the various observational criteria that we imposed is very short. Only observing the site of a SN Ic having potentially a more massive progenitor system might bear fruit — in fact, observations with *HST* are pending (GO-14075, PI: O. Fox) to image deeply the site of the broad-lined SN Ic 2002ap (e.g., Mazzali et al. 2002) in Messier 74 (NGC 628) in these same two UV bands.

The example of SN 1994I illustrates the value of deep searches at the sites of SNe at very late times, motivating future efforts to obtain deep limits for additional examples and to statistically model the properties of core-collapse SNe.

We appreciate the helpful comments from the anonymous referee. The authors are also very grateful to Robert Izzard for numerous discussions and for allowing the use of his code *binary_c*. We are also appreciative of discussion with Maria Drout regarding the SN 1994I light and color curves, and with Sung-Chul Yoon regarding his models. Based on observations made with the NASA/ESA *Hubble Space Telescope*, obtained at the Space Telescope Science Institute, which is operated by the Association of Universities for Research in Astronomy, Inc., under NASA contract NAS 5-26555. These observations are associated with and supported by program GO-13340. De Mink acknowledges support by a Marie Skłodowska-Curie Reintegration Fellowship (H2020-MSCA-IF-2014, project id 661502) awarded by the European Commission.

Facilities: HST (WFC3, WFPC2).

REFERENCES

- Aasi, J., Abadie, J., Abbott, B. P., et al. 2013, *Phys. Rev. D*, 88, 062001
- Alexander, K. D., Soderberg, A. M., & Chomiuk, L. B. 2015, *ApJ*, 806, 106
- Baron, E., Hauschildt, P. H., Branch, D., Kirshner, R. P., & Filippenko, A. V. 1996, *MNRAS*, 279, 799
- Barth, A. J., Van Dyk, S. D., Filippenko, A. V., Leibundgut, B., & Richmond, M. W. 1996, *AJ*, 111, 2047
- Bianco, F. B., Modjaz, M., Hicken, M., et al. 2014, *ApJS*, 213, 19
- Calzetti, D., Lee, J. C., Sabbi, E., et al. 2015, *AJ*, 149, 51
- Cao, Y., Kasliwal, M. M., Arcavi, I., et al. 2013, *ApJ*, 775, L7
- Cardelli, J. A., Clayton, G. C., & Mathis, J. S. 1989, *ApJ*, 345, 245
- Castelli, F., & Kurucz, R. L. 2003, *Modelling of Stellar Atmospheres*, 210, 20P
- Claeys, J. S. W., de Mink, S. E., Pols, O. R., Eldridge, J. J., & Baes, M. 2011, *A&A*, 528, A131
- Chevalier, R. A. 1984, *Annals of the New York Academy of Sciences*, 422, 215
- Chevalier, R. A., & Fransson, C. 1994, *ApJ*, 420, 268
- Chevalier, R. A., & Fransson, C. 2006, *ApJ*, 651, 381

⁵ <http://etc.stsci.edu/etc/input/wfc3uvis/imaging/>

- Clocchiatti, A., Wheeler, J. C., Kirshner, R. P., et al. 2008, *PASP*, 120, 290
- Crockett, R. M., Smartt, S. J., Eldridge, J. J., et al. 2007, *MNRAS*, 381, 835
- Crockett, R. M., Maund, J. R., Smartt, S. J., et al. 2008, *ApJ*, 672, L99
- de Mink, S. E., Langer, N., Izzard, R. G., Sana, H., & de Koter, A. 2013, *ApJ*, 764, 166
- Dewi, J. D. M., & Tauris, T. M. 2000, *A&A*, 360, 1043
- Dolphin, A. E. 2000, *PASP*, 112, 1383
- Drout, M. R., Soderberg, A. M., Gal-Yam, A., et al. 2011, *ApJ*, 741, 97
- Duchêne, G., & Kraus, A. 2013, *ARA&A*, 51, 269
- Ekström, S., Georgy, C., Eggenberger, P., et al. 2012, *A&A*, 537, A146
- Eldridge, J. J., Izzard, R. G., & Tout, C. A. 2008, *MNRAS*, 384, 1109
- Eldridge, J. J., Fraser, M., Smartt, S. J., Maund, J. R., & Crockett, R. M. 2013, *MNRAS*, 436, 774
- Elias-Rosa, N., Pastorello, A., Maund, J. R., et al. 2013, *MNRAS*, 436, L109
- Elmhamdi, A., Danziger, I. J., Branch, D., et al. 2006, *A&A*, 450, 305
- Ergon, M., Sollerman, J., Fraser, M., et al. 2014, *A&A*, 562, A17
- Folatelli, G., Bersten, M. C., Benvenuto, O. G., et al. 2014, *ApJ*, 793, L22
- Fox, O. D., Azalee Bostroem, K., Van Dyk, S. D., et al. 2014, *ApJ*, 790, 17
- Gal-Yam, A., Fox, D. B., Kulkarni, S. R., et al. 2005, *ApJ*, 630, L29
- Georgy, C., Meynet, G., Walder, R., Folini, D., & Maeder, A. 2009, *A&A*, 502, 611
- Hamann, W.-R. and Koesterke, L. and Wessolowski, U., 1995, *A&A*, 229, 151
- Hobbs, G. and Lorimer, D. R. and Lyne, A. G. and Kramer, M., 2005, *MNRAS*, 360, 974
- Ho, L. C., & Filippenko, A. V. 1995, *ApJ*, 444, 165
- Hurley, J. R., Pols, O. R., & Tout, C. A. 2000, *MNRAS*, 315, 543
- Hurley, J. R., Tout, C. A., & Pols, O. R. 2002, *MNRAS*, 329, 897
- Immler, S., Pietsch, W., & Aschenbach, B. 1998, *A&A*, 336, L1
- Immler, S., Wilson, A. S., & Terashima, Y. 2002, *ApJ*, 573, L27
- Iwamoto, K., Nomoto, K., Höflich, P., et al. 1994, *ApJ*, 437, L115
- Izzard, R. G., Tout, C. A., Karakas, A. I., & Pols, O. R. 2004, *MNRAS*, 350, 407
- Izzard, R. G., Dray, L. M., Karakas, A. I., Lugaro, M., & Tout, C. A. 2006, *A&A*, 460, 565
- Izzard, R. G., Glebbeek, E., Stancliffe, R. J., & Pols, O. R. 2009, *A&A*, 508, 1359
- Kasen, D. 2010, *ApJ*, 708, 1025
- Kim, C., Kalogera, V., & Lorimer, D. 2010, *NewAR*, 54, 148
- Kim, H.-J., Yoon, S.-C., & Koo, B.-C. 2015, *ApJ*, 809, 131
- Kouwenhoven, M. B. N., Brown, A. G. A., Portegies Zwart, S. F., & Kaper, L. 2007, *A&A*, 474, 77
- Kroupa, P. 2001, *MNRAS*, 322, 231
- Lee, M. G., Kim, E., Kim, S. C., et al. 1995, *Journal of Korean Astronomical Society*, 28, 31
- Li, W., Leaman, J., Chornock, R., et al. 2011, *MNRAS*, 412, 1441
- Liu, Z.-W., Tauris, T. M., Roepke, F. K., et al. 2015, *A&A*, in press (arXiv:1509.03633)
- Mason, B. D., Hartkopf, W. I., Gies, D. R., Henry, T. J., & Helsel, J. W. 2009, *AJ*, 137, 3358
- Maund, J. R., Smartt, S. J., Kudritzki, R. P., Podsiadlowski, P., & Gilmore, G. F. 2004, *Nature*, 427, 129
- Maund, J. R., Smartt, S. J., & Schweizer, F. 2005, *ApJ*, 630, L33
- Maund, J. R., Arcavi, I., Ergon, M., et al. 2015, *MNRAS*, 454, 2580
- Mazzali, P. A., Deng, J., Maeda, K., et al. 2002, *ApJ*, 572, L61
- Moriya, T. J., Liu, Z.-W., & Izzard, R. G. 2015, *MNRAS*, 450, 3264
- Nieuwenhuijzen, H. and de Jager, C., 1990 *A&A*, 231, 134
- Nomoto, K., Yamaoka, H., Pols, O. R., et al. 1994, *Nature*, 371, 227
- Öpik, E. 1924, *Tartu Obs. Publ.*, 25, 6
- Paxton, B., Marchant, P., Schwab, J., et al. 2015, *ApJS*, 220, 15
- Podsiadlowski, P., Joss, P. C., & Hsu, J. J. L. 1992, *ApJ*, 391, 246
- Pols, O. R., & Dewi, J. D. M. 2002, *PASA*, 19, 233
- Pols, O. R. and Schröder, K.-P. and Hurley, J. R. and Tout, C. A. and Eggleton, P. P. 1998, *MNRAS*, 298, 525
- Rampadarath, H., Morgan, J. S., Soria, R., et al. 2015, *MNRAS*, 452, 32
- Richardson, D., Branch, D., & Baron, E. 2006, *AJ*, 131, 2233
- Richmond, M. W., Van Dyk, S. D., Ho, W., et al. 1996, *AJ*, 111, 327
- Sana, H., de Mink, S. E., de Koter, A., et al. 2012, *Science*, 337, 444
- Sasaki, M., Kosugi, G., Ishigaki, T., et al. 1994, *PASJ*, 46, L187
- Sauer, D. N., Mazzali, P. A., Deng, J., et al. 2006, *MNRAS*, 369, 1939
- Schlafly, E. F., & Finkbeiner, D. P. 2011, *ApJ*, 737, 103
- Smith, N., Li, W., Filippenko, A. V., & Chornock, R. 2011, *MNRAS*, 412, 1522
- Tonry, J. L., Dressler, A., Blakeslee, J. P., et al. 2001, *ApJ*, 546, 681
- Tout, C. A., Aarseth, S. J., Pols, O. R., & Eggleton, P. P. 1997, *MNRAS*, 291, 732
- Tramper, F., Straal, S. M., Sanyal, D., et al. 2015, *A&A*, 581, A110
- Van Dyk, S. D., Li, W., & Filippenko, A. V. 2003, *PASP*, 115, 1
- Vink, J. S. and de Koter, A. and Lamers, H. J. G. L. M. 2000 *A&A*, 362, 295
- Vinkó, J., Takáts, K., Szalai, T., et al. 2012, *A&A*, 540, A93
- Webbink, R. F., 1984, *ApJ*, 277, 355
- Wellons, S.; Soderberg, A. M.; Chevalier, R. A. 2012, *ApJ*, 752, 17
- Weiler, K. W., Panagia, N., Stockdale, C., et al. 2011, *ApJ*, 740, 79
- Wheeler, J. C., Harkness, R. P., Clocchiatti, A., et al. 1994, *ApJ*, 436, L135
- Woosley, S. E., Langer, N., & Weaver, T. A. 1993, *ApJ*, 411, 823
- Woosley, S. E., Langer, N., & Weaver, T. A. 1995, *ApJ*, 448, 315
- Woosley, S. E., & Bloom, J. S. 2006, *ARA&A*, 44, 507
- Yokoo, T., Arimoto, J., Matsumoto, K., Takahashi, A., & Sadakane, K. 1994, *PASJ*, 46, L191
- Yoon, S.-C., Woosley, S. E., & Langer, N. 2010, *ApJ*, 725, 940
- Yoon, S.-C., Gräfener, G., Vink, J. S., Kozyreva, A., & Izzard, R. G. 2012, *A&A*, 544, L11
- Young, T. R., Baron, E., & Branch, D. 1995, *ApJ*, 449, L51
- Zahn, J.-P., 1977, *A&A*, 57, 383